Charge-carrier mobilities in superfluid helium under pressure*

Burton Brody[†]

H. M. Randall Laboratory of Physics, The University of Michigan, Ann Arbor, Michigan 48104

(Received 25 February 1974; revised manuscript received 4 September 1974)

Data are presented for the mobilities of the positive and negative charge carriers, and the ratios of these, in superfluid helium, from 1.2 K through the λ line and from the vapor pressure to the freezing curve.

I. INTRODUCTION

Manipulating charge carriers in He II provides a means of exploring both the dispersion relation of the quasiparticle spectrum and the structures of the carriers themselves. In 1958, Meyer and Reif[1] first investigated the mobility of ions in superfluid helium under the influence of a weak electric field and interpreted their data in terms of scattering by the normal fluid. Similar experiments have followed and the technique has been improved. Precise mobility data now exist from tenths of a degree to several degrees at the vapor pressure,[2] and at higher pressures (to the freezing curve and in the solid), both at lower temperatures, where the phonon interactions predominate and the number densities of quasiparticles are small (so their interactions may be neglected) and near the λ line.[3-6] The phonon scattering of the negative carrier is now fairly well understood,[5,7] and attention has now focused on the roton interactions.[6-11] This paper presents intensive data on the mobilities of both positive and negative charge carriers and the ratios of these from the vapor pressure to the freezing curve, from 1.2 K to the λ line, as shown in Fig. 1. Agreement of these data where they overlap others is very good,[2,3,5,6] so that these data form a link from the vapor pressure to the freezing curve, from millikelvin to beyond the λ line.

II. APPARATUS AND TECHNIQUE

Mobilities are deduced from the time of flight of a pulse of charges through a drift space under the influence of a weak electric field. If the field E imparts much less than thermal energy to a charge carrier between collisions, and if the carrier takes time τ to traverse distance L under the potential difference $V = EL$, the zero-field mobility μ is defined as the limiting ratio of drift speed v to applied field E,

$$\mu = \lim_{E \to 0} \frac{v}{E} = \frac{L/\tau}{V/L} = \frac{L^2}{V} \tau^{-1}.$$

If the data are expressed in terms of a friction coefficient

$$\Gamma = F/v = e/\mu,$$

where the force is given by $F = eE$, this friction coefficient can be analyzed as a sum of contributions from different types of scatterers—phonons, rotons, and He³.

A. Apparatus

The experimental system developed for this measurement has been presented in greater detail elsewhere,[12] and has by now become entirely standard. The set of electrodes diagrammed to scale in Fig. 2 was oriented vertically with the collector at the top. The bottom three disks held a radioactive source to ionize the ambient helium and nucleate the carriers, a source grid to extract carriers of a particular sign, and a gate grid to admit these carriers at a given instant into the drift region. The drift region, with two internal electrodes to secure electric field homogeneity, terminated in a collector (Frisch) grid which electrostatically shielded the collector just beyond it. A retarding field in the gate region was periodically overridden by a gating pulse which lifted the potential of the first two electrodes to create an accelerating field in all regions.

The drift distance was 5.39 cm at our operating temperatures and pressures. The electrode windows were 0.95 cm in diameter and screened with 200 wires/in., so interregion field penetration was inconsequential. Electrostatic charging of critical surfaces and significant field inhomogeneities were also eliminated.

The electrode assembly was mounted in a sealed brass can with stainless-steel electrical-access tubes and a 5 ft. long, $\frac{1}{16} \times 0.004$-in. wall, coiled Cupronickel fill capillary. A twisted Manganin wire loop introduced through the wall of the capillary, about 1 ft. from the lower end and 7 in. above the can flange, could heat the entrant helium from that point to just inside the can, to melt or prevent plugs of frozen helium.

B. Pressure and temperature

The experimental helium was pressurized through the capillary connecting the can to an external gas-handling system which included a 500-psi (absolute) gauge and a high-pressure helium-gas cylinder.
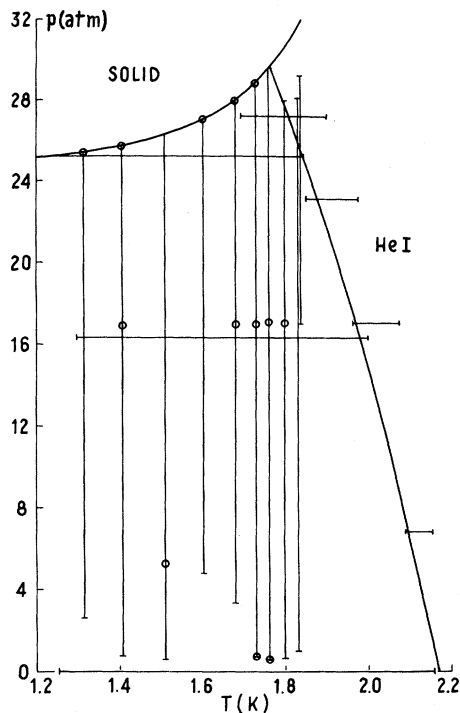
FIG. 1. Region of the p-T space investigated in this experiment. Each straight line represents a data run. Circles mark the locations of $v(E)$ plots.

The cylinder furnished both the condensable gas and the applied pressure. The pressure gauge was calibrated with a dead-weight tester to ± 0. 5 psi, and *in situ* observations on a given datum repeated under different cycles of increasing and decreasing pressure fell within the gauge's rated hysteresis of ± 0. 1 psi.

The capillary passed from superfluid temperatures at the bottom of the Dewar to room temperature at the top, but hydrostatic and fountain-effect pressure heads introduced probable errors of much less than 0. 1 psi.

Temperatures were determined from Octoil and mercury manometers connected to the Dewar pumping head and from a resistor thermometer (Allen-Bradley 100 Ω, $\frac{1}{2}$ W) in a thermostatting feedback loop with a wire-wound resistor heater just above the experimental can. Dissipation of 10^{-9}–10^{-10} W in the thermometer (a power level observed to not affect the resistance) accommodated thermostatting to better than 0. 5 mK. The bulk thermal resistance of the brass can at 2 °K and the Kapitza boundary resistances at the surfaces could generate no more than a few millikelvin difference between the bath and the can interior for any reasonable heat flows out through the can wall, so the determined temperatures were at worst a few millikelvin cooler than the cell interior. At

the relatively high temperatures explored here, and with our minimal heat inflow, the difference in vapor pressure between the manometer inlet at the pumping flange and the liquid surface also introduced at most a few millikelvin difference in temperature.

Higher temperatures were read to within 2 mK with the manometers. It was noted that the density of the Octoil varied over time, but this introduced an error of no more than 3 mK at 1. 3 K to 4 mK at 1. 83 K. A correction of some of the recorded pressures by addition of 0. 2 cm Octoil to compensate for inadequate pumping of the low-pressure side of the manometer introduced a maximum uncertainty of less than 5 mK at 1. 3 K. Lower temperatures were determined with the resistance thermometer by interpolating in a linear plot of log (R) vs log (oil height).

Combining these considerations our uncertainties become ± 7 mK and ± 0. 4 psi. The phase boundaries extracted from our data by methods described hereinafter agree extremely well within these errors with those of Grilly and Grilly and Mills,[13] as shown in Fig. 3, with the possibility, consistent with the considerations just given, that our lowest temperatures may be a few millikelvin low.

III. PROCEDURES

A. Operation

For each run a $3\frac{1}{2}$-h condensation of gas in the capillary evaporated less than a liter of liquid from the bath to collect 0. 2 l in the experimental can. When the can was full of liquid (on the indication that the pressure-gauge reading would suddenly rise—when the gas flow stopped), voltages were turned on and a mobility signal appeared.

The source field was set at about 500 V/cm to give a current at the vapor pressure and the lowest temperatures of about 10^{-11} A. Variation below this current level had no effect on the current pulse
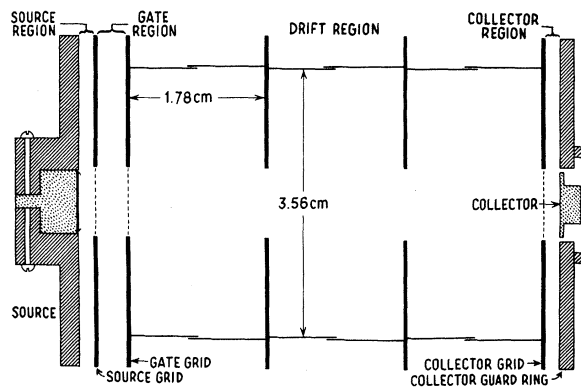

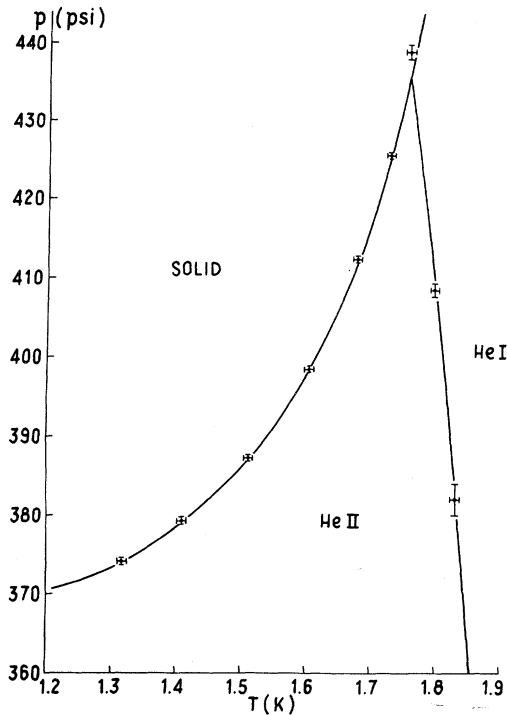FIG. 2. Time-of-flight electrode assembly, to scale.

FIG. 3. Points on the phase boundaries determined in this experiment (indicated by points with error bars) compared with those of Ref. 13 (represented by solid lines).

shape and, more particularly, the measured transit time. The observed current pulses were usually much less than 10^{-11} A, since the current decreases with the mobility: at the highest pressures and at high temperatures the mobilities and currents were down by two orders of magnitude.

The drift field was generally maintained at about 100 V/cm, although it was periodically scanned from 50–120 V/cm, as described hereinafter. The gate and collector fields were set approximately equal to the drift field although significant variation of the gate and collector fields and different combinations of gate pulse and back bias for a given net gate field had no observable effect on the transit times.

For each datum the time range and the number of sweeps accumulated in a multichannel pulse-height analyzer/time-averaging computer (CAT) were selected to define the features of the trace to within one percent of the transit time. Fluctuations or drift of the temperature and pressure during an accumulation were nearly always much less than would cause a one-percent change in mobility: very few of the data for which this was not so were retained.

Most of the data were collected for the pairs of

carriers in alternating order at successive points stepping along an isobar or isotherm. After a reversal of field polarity to switch carriers, the signal would grow to full size in a minute or two with a constant exhibited transit time. Since each carrier had alternately the long time while temperature or pressure was changing or the short time after a field reversal to come to equilibrium, incomplete field equilibration or static charging effects would have generated a wiggle in the data: no such wiggle was seen. This paired data taking insured for the two carriers identical temperatures and pressures in sensitive areas.

B. Temperature and pressure

Pressure and temperature were changed slowly— perhaps 15 min to increase 50 psi at lower pressures[14] and much longer for significant changes in temperature. Most of the data were collected along isotherms. A few isobaric sequences confirmed the pressure equilibration and the thermometry of the isotherms. The isobars also covered more carefully the regions where the mobility was varying rapidly with temperature and extended the data through the λ line.

Along the isotherms, the freezing point was usually associated with the pressure gauge remaining at some value and the mobility signal eventually disappearing despite continued gas inflow. To read this freezing pressure, the gas flow was momentarily stopped, before or after the signal disappeared. This value was also the pressure at which the signal reappeared when gas was pumped out: melting and freezing pressures were the same to within 0.1 psi.

Instead of sticking, below 1.6 K the gauge would oscillate about a constant pressure at about 3 Hz with a 0.4 psi excursion for a typical gas flow. The oscillation apparently set in just at the freezing pressure, stopping only when the gas flow was stopped or when presumably the can contents were frozen. For the 1.5 K isotherm the onset of oscillation was accepted as adequate indication of the phase boundary. Above 1.7 K with reasonable gas-flow rates the capillary would freeze before the freezing pressure was reached in the can. The heater in the lower end of the capillary did appear to break plugs, but reaching the freezing pressure in the can was a tedious procedure above 1.7 K.

The other phase boundary, the λ line, was correlated with a characteristic change in the isothermal curves of the mobilities of both carriers and their ratios. Characteristic changes in the isobaric curves, located less accurately, agree with these determinations. As shown in Fig. 3, such phase-boundary determinations agree very well with those of Grilly and Grilly and Mills.[13]
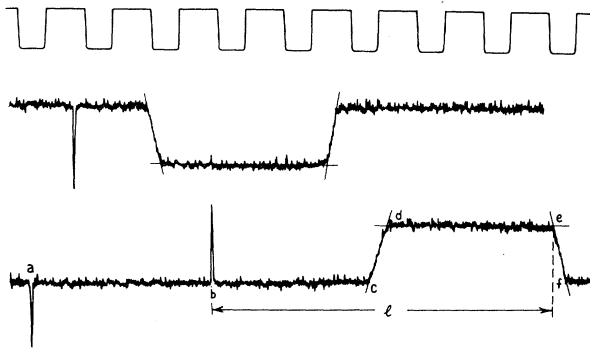
FIG. 4. Representative traces of a time calibration (0.1 sec/cycle) and 49-sweep accumulations of the time of flight for the positive and negative carrier ($l = 5.34$ in. for the positive carrier on the original, at 240 psi and 1.54 K). Superimposed letters label salient points on the traces.

C. Mobility

For each value of temperature and pressure the two carrier transit times in a field of about 100 V/cm were recorded. To confirm that we remained in the zero-field regime, at several values of temperature and pressure, as indicated in Fig. 1, times of flight were measured for each carrier at five drift fields (and corresponding gate and collector fields) from 50 to 120 V/cm. Straight lines fit the graphs of inverse time of flight (proportional to velocity) versus field quite well but randomly missed the origin[15] by amounts frequently outside reasonable error. Extraneous voltages in the cell, as from charged contaminant layers on the electrodes or from space charge,[6] could have had this effect, but we could find no correlation of this phenomenon with time, polarity, or any other variable. In any case, the difference between the slope on a $v(E)$ plot of the best-fit straight line and the ratio v/E for the 500-V point was never more than 5%. This was greater than the maximum difference between independent determinations at a given temperature and pressure so we assigned to our mobilities an uncertainty of ± 5%. This is conservative: internal consistency of the data and agreement with the mobility data of others suggest a probable error closer to 2 or 3%.[2,3]

For each datum a normal accumulated trace showed two spikes in opposite directions near the beginning and a trapezoid about as wide as the space between the spikes at the end. Figure 4 presents a typical trace with salient points labelled. Spikes a and b mark the opening and closing of the gate. The leading face cd of the trapezoid begins when the front edge of the charge pulse passes the collector grid and ends when it reaches the collector, while

ef at the other end of the trapezoid plateau marks the same transit of the collector space for the trailing edge of the pulse. The signal plateau de is constant while the cylinder of charge, filling the collector space, is received at the collector.

Enough sweeps were averaged to define the distance be in Fig. 4 to one percent. In the very few cases where variations in pulse shape precluded superposition of a simple, measurable trapezoid, the datum was discarded. The observed dimensions and characteristics of the received signal could be completely explained in terms of a moving cylinder of charge without noticeable effects of diffusion or electrostatic spreading. The leading face cd traverses the gate region while the trailing face ef does not: large changes in the gate and source fields could affect slightly the time of flight measured to the front edge of the trapezoid, but the trailing edge is insensitive, so the mobility was determined from the length $l = be$ from the drift field alone. The mobility is $\mu = L^2/V\tau$, where τ is l times a scale factor involving time calibrations. Tabulations of all the mobility and mobility-ratio data are available through the NAPS depository[16]; Figs. 5–11 summarize the data with isothermal and isobaric families of curves for each carrier and for the ratios.
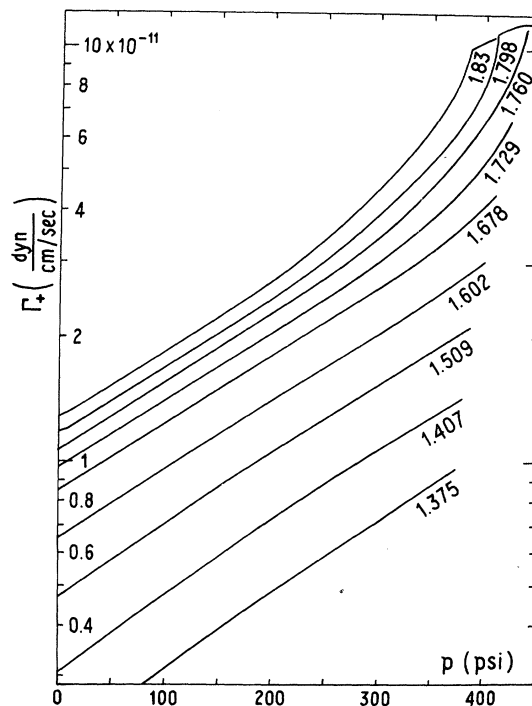

FIG. 5. Smoothed isothermal curves of the friction-coefficient data for the positive carrier versus applied pressure.
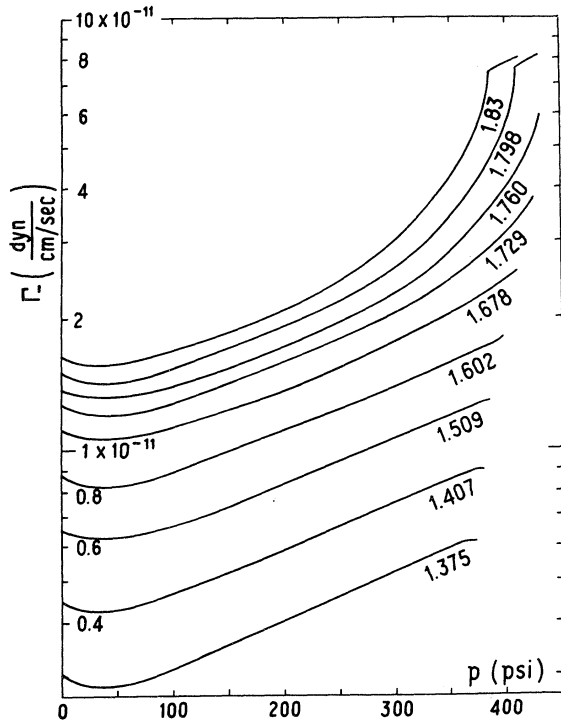
FIG. 6. Smoothed isothermal curves of the friction-coefficient data for the negative carrier versus applied pressure.

IV. INTERPRETATIVE REMARKS

The friction coefficient represents a sum of inhibitions to the charge-carrier drift due to collisions with the scatterers of the ambient fluid: in
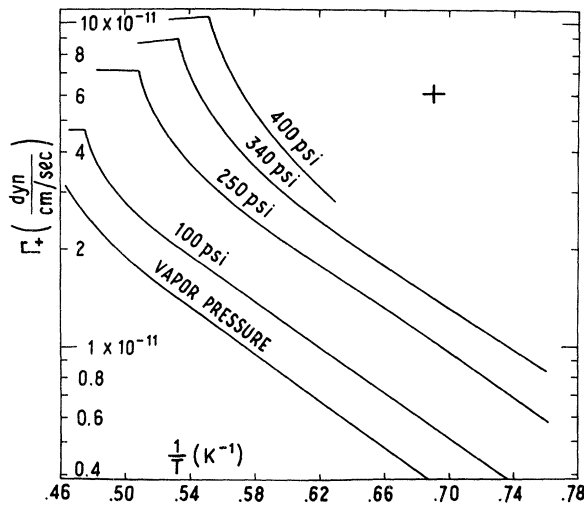

FIG. 7. Smoothed isobaric curves of the friction-coefficient data for the positive carrier versus inverse temperature.
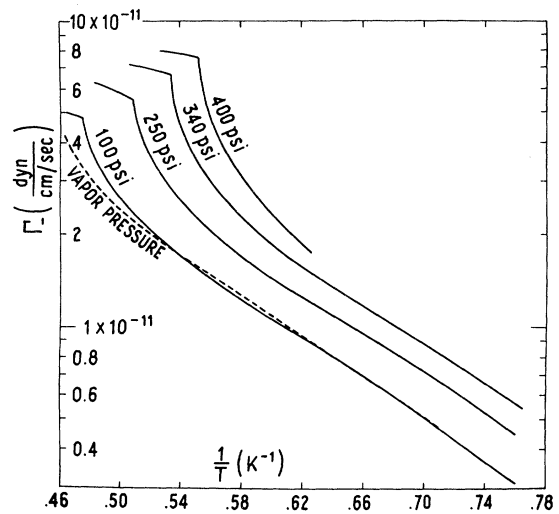

FIG. 8. Smoothed isobaric curves of the friction-coefficient data for the negative carrier versus inverse temperature.

the temperature range of our data rotons dominate the scattering, with phonons contributing at most a few percent. Extending the phonon-scattering models from below 1 K to higher temperatures permits
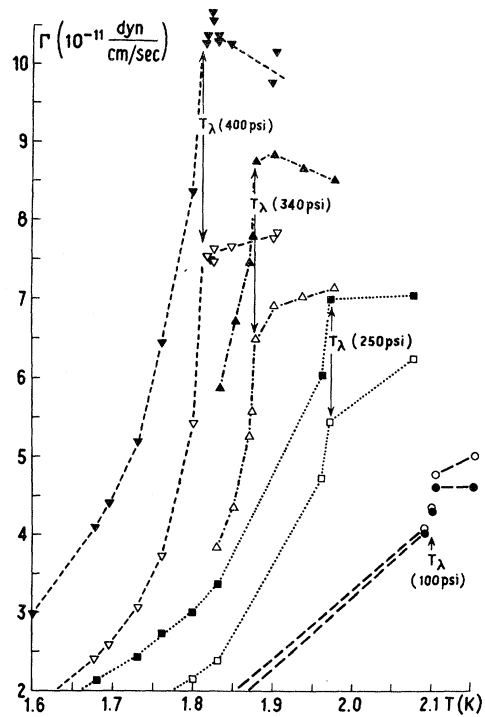

FIG. 9. Isobaric data for both carriers near the λ line. Closed and open symbols designate the positive and negative carriers, respectively; the lines are guides to the eye. The location of the λ temperature at each pressure is from Grilly (Ref. 13).
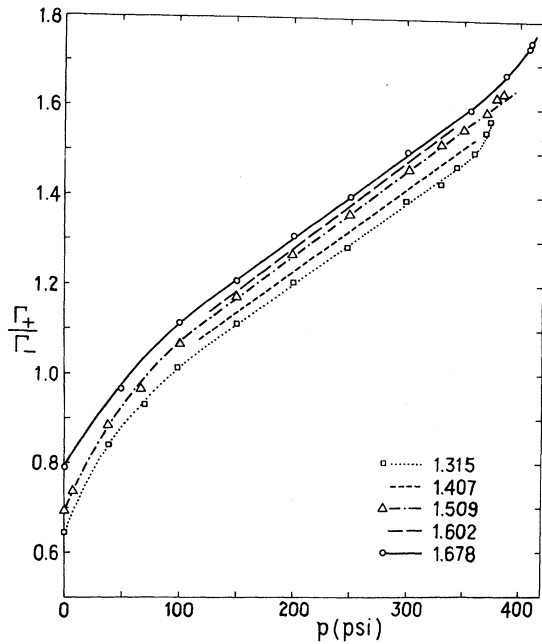
FIG. 10. Ratios of the positive-to-negative friction coefficient versus pressure for temperatures up to T = 1678 K. Data are shown on three complete curves; intermediate isothermal sequences of data are schematically represented by abbreviated lines.

approximate isolation of the roton scattering: the phonon contribution to the friction coefficient is calculated[8] to be about 2% at 1.0 K and $\frac{1}{2}$% at 1.7 K for the positive carrier, and 15% at 1.0 K (and decreasing more slowly) for the negative carrier. The phonon contribution decreases at higher pressures as well.[5]

At the lower temperatures our mobilities should conform to a roton-carrier kinetic-theory interaction, involving roton number densities and roton-carrier scattering cross sections[8]: isobaric curves of our data for each carrier versus inverse temperature are dominated by the exponential dependence of the roton number density on temperature, up to higher temperatures where a kinetic-theory model should no longer apply. At the higher temperatures the roton number density becomes so large that the roton-carrier interaction should be describable by viscous hydrodynamics in terms of a friction coefficient given from Stokes's law as $\Gamma_{\pm} = A_{\pm}\pi\eta R_{\pm}$, for viscosity η, carrier scattering radius $R_{\pm}$, and a coefficient taken to be $A_{+} = 6$ and $A_{-} = 4$ for the two carriers.[3,17,18] This interpretation is clearly oversimplified,[19] but with these coefficients $A_{\pm}$, since the ratio of the mobilities at the vapor pressure is seen to be 0.76 ± 0.02 from $T = 1.69$–2.16 °K, the implied ratio of the charge-carrier scattering radii would be close to 2.0 at

the vapor pressure in the viscous regime.

The transition from a kinetic theory to a viscous hydrodynamics occurs when the roton-roton mean free path becomes comparable to the carrier sizes. Figure 12 presents loci of constant roton mean free path, calculated for a δ-function interaction[20] as $l_{\rho} = v_{\rho}t_{\rho}$, where $v_{\rho} = (kT/m_{\rho})^{1/2}$ and

$$t_{\rho} = [15(2\pi)^{3/2}/2\hbar](\hbar/p_{0})^{4}e^{\Delta/kT}\eta_{\rho}$$

in terms of roton effective mass m_{ρ}, momentum p_{0}, and energy gap Δ, and the roton contribution η_{ρ} to the normal-fluid viscosity, where we have extracted η_{ρ} from heat-flow measurements[21] and estimated $\Delta(\rho, T)$ from neutron scattering data.[22] We emphasize not the quantitative accuracy of these curves,[9] but their qualitative features. Dahm and Sanders[18] located the kinetic-theory-viscous-hydrodynamics transition for the positive carrier at $T = 2.0$ K at the vapor pressure, and this transition should be traceable to higher pressures. Characteristic features of the families of curves, particularly in Fig. 11, appear to follow locus curves in Fig. 12.

In both regimes the mobility combines properties of the rotons and the charge carriers. The bubble model of the negative carrier—a cavity hollowed out around a single electron to minimize the system free energy—has been substantiated by a variety of experiments,[23] including mobility measurements in the phonon-limited domain.[5,7,8] Experi-
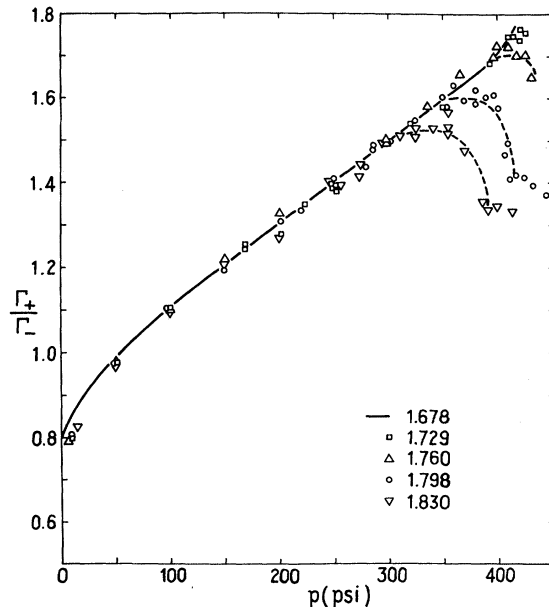

FIG. 11. Ratios of the positive-to-negative friction coefficient versus pressure for temperatures above 1.678 K. The solid line retraces the 1.678 K curve from Fig. 10, while the dashed lines are guides to the eye for isothermal sequences at higher temperatures.
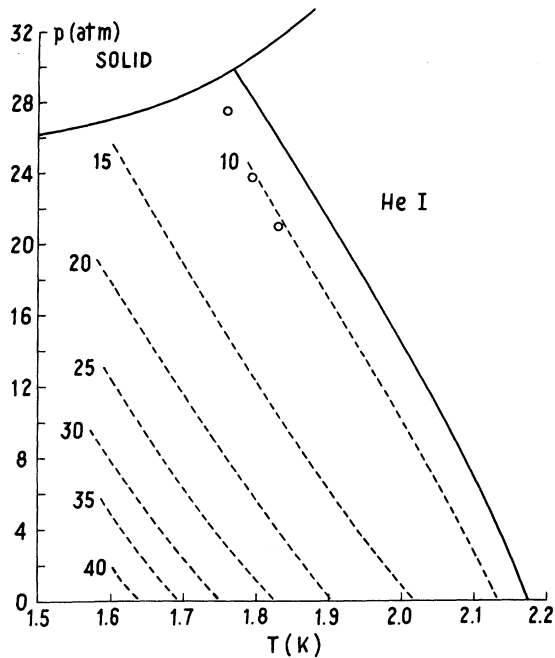
FIG. 12. Loci of constant roton mean free path, as calculated from Khalatnikov (Ref. 19). Circles mark a distinctive transition in the isothermal curves of the mobility ratios.   ✦

mental confirmation of the snowball model[24] for the positive carrier, however, is less clear. The positive-carrier effective mass and radius deduced from several experiments[5,7,8,23] are consistent with the predictions of the model, but whereas the surface tension of the bubble skin is a minor feature, the poorly known liquid-solid surface tension σ_{ls} plays an important role for the snowball. With no surface tension the snowball would grow indefinitely as the ambient pressure approached freezing, while $\sigma_{ls} = 0.135$ erg cm^2, as inferred by Schwarz from vapor pressure mobility measurements,[7] would keep the snowball radius to a few angstroms.

Ratios of the carrier mobilities can deemphasize many of the scattering-fluid features to emphasize relative properties of the two carriers, alone. The regularities in Figs. 10 and 11, especially when accommodation is made for the several-percent phonon contribution to the scattering of the negative carrier, support this expectation. As shown, while the constituent mobilities change by factors of more than ten, the mobility ratio ranges from less than 0.7 at the vapor pressure to unity at 4–6 atm (at different temperatures), to slightly more than 1.7 at the freezing curve. In the viscous regime the mobility ratio should reduce to essentially the relative roton scattering radii of the two carriers, while in the kinetic-theory regime it should

be basically the ratio of the mean roton-carrier scattering cross sections. On these grounds it is apparent from Figs. 10 and 11 that provided that the negative carrier does nothing anomalous, in neither regime is there evidence for dramatic growth of the snowball approaching the freezing pressure. Although the analysis is tenuous, it is interesting that the mobilities are equal at temperatures and pressures where the models would indicate the carrier radii themselves to differ by a factor of almost 2.

At the lower temperatures (Fig. 10) the isothermal sequences of mobility ratios form a family of curves, each increasing linearly with pressure in midrange and showing the effect of the initial compression of the bubble at low pressures. Above about 1.68 K this family degenerates into a single curve, even though the constituent mobilities are changing by factors of up to 2. Subtraction of the phonon contribution to the negative-carrier friction coefficient should only slightly change this picture, particularly at higher pressures and the higher temperatures. Above about 1.73 K individual curves peel off this common curve, in a characteristic way, along a locus of constant roton mean free path, as presented in Fig. 12, atmospheres below freezing, but apparently at higher pressures than the presumed kinetic-viscous transition for the positive carrier. Finally, the discontinuity in the slopes of the 1.8 K and 1.83 K ratio curves was identified with the λ line.

V. SUMMARY

Our data, agreeing well with measurements at both higher and lower temperatures, present an accurate survey of the mobilities of the basic positive and negative charge carriers at the higher temperatures in He II. The mobilities and their ratios provide information on the charge carriers, the rotons, and their interactions, including indication that the positive charge carrier does not grow dramatically approaching freezing. The data present interesting detail which a successful model of the charge carriers and the roton interactions must accommodate.

ACKNOWLEDGMENTS

*Work supported in part by the U. S. Atomic Energy Commission and the National Science Foundation.

†Current address: Bard College, Annandale-on-Hudson, NY 12504.

[1]L. Meyer and F. Reif, Phys. Rev. 110, 297 (1958).

[2]K. W. Schwarz and R. W. Stark, Phys. Rev. Lett. 21, 967 (1968); K. W. Schwarz, Phys. Rev. A 6, 837 (1972).

[3]G. Ahlers and G. Gamota, Phys. Lett. A 38, 65 (1972).

[4]K. O. Keshishev, Yu. Z. Kovdrya, L. P. Mezhov-Deglin, and A. I. Shal'nikov, Zh. Eksp. Teor. Fiz. 56, 94 (1969) [Sov. Phys.-JETP 29, 53 (1969)].

[5]R. M. Ostermeier, Phys. Rev. A 8, 514 (1973).

[6]D. Goodstein, A. Savoia, and F. Scaramuzzi, Phys. Rev. A 9, 2151 (1974).

[7]K. W. Schwarz, Phys. Rev. A 6, 1958 (1972), and references therein.

[8]R. Barera and G. Baym, Phys. Rev. A 6, 1558 (1972), and references therein.

[9]J. Ruvalds, Phys. Rev. Lett. 27, 1769 (1971), and references therein.

[10]R. M. Bowley, J. Phys. C 4, 1645 (1971).

[11]A. K. Rajagopal, A. Bagchi, and J. Ruvalds, Phys. Rev. A 9, 2707 (1974).

[12]B. A. Brody, Ph. D. thesis (University of Michigan, 1970)(unpublished), available through University Microfilms, North Zeeb Road, Ann Arbor, Mich.

[13]E. R. Grilly and R. L. Mills, Ann. Phys. (N.Y.) 18, 250 (1962); E. R. Grilly, Phys. Rev. 149, 97 (1972).

[14]Equilibration after a change of pressure was a matter of minutes at most. Ostermeier has suggested that his indication in Ref. 5 of 1–2 h is unwarranted.

[15]We did not observe the uniform deviation observed by Schwarz.

[16]See NAPS document No. 02486 for 8 pages of supplementary material. Order from ASIS/NAPS c/o Microfiche Publications, 440 Park Avenue South, New York, N.Y. 10016. Remit in advance for each NAPS accession number, $1.50 for microfiche or $5.00 for photocopies up to 30 pages, 15¢ for each additional page. Make checks payable to Microfiche Publications.

[17]K. W. Schwarz, Phys. Rev. A 5, 2510 (1972).

[18]A. J. Dahm and T. M. Sanders, Jr., Phys. Rev. Lett. 17, 126 (1962).

[19]R. M. Ostermeier and K. W. Schwarz, Phys. Rev. A 5, 2510 (1972).

[20]I. M. Khalatinikov, *Introduction to the Theory of Superfluidity* (Benjamin, New York, 1965), pp. 49 and 127.

[21]D. F. Brewer and D. O. Edwards (a) in *Proceedings of the Eighth International Conference on Low Temperature Physics*, edited by R. O. Davies (Butterworths, London, 1963), p. 96; (b) Proc. R. Soc. A 251, 247 (1959); (c) Philos. Mag 7, 721 (1962).

[22]B. A. Brody, in Ref. 12, Sec. Va.

[23]J. Poitrenaud and F. I. B. Williams, Phys. Rev. Lett. 29, 1230 (1972).

[24]K. R. Atkins, Phys. Rev. 116, 1339 (1959).